Single-Cycle Non-Sequential Double Ionization

Boris Bergues, Matthias Kübel, Nora G. Kling, Christian Burger, and Matthias F. Kling

(Invited Paper)

***Abstract*—Non-sequential double ionization (NSDI) is a process in which two electrons are ripped off an atom or molecule by a strong laser field in a correlated manner. Although NSDI has been the subject of numerous experimental and theoretical studies over the past three decades, the exact mechanisms responsible for the observed energy and momentum sharing between the electrons generated in the process, are not yet fully understood. The main reason lies in the fact that the theoretical description of the complex correlated many body dynamics that govern NSDI is exceedingly difficult. A particularly challenging task for theory is the modeling of NSDI dynamics over time scales exceeding one period of the laser field. As a result, most calculations are restricted to a single laser cycle. On the experimental side, in contrast, kinematically complete experiments on single-cycle NSDI has long been prohibitively challenging. Therefore, the comparison between theory and experiments has been limited, so far, to a very qualitative level. We review recent results obtained from first kinematically complete NSDI experiments in the single cycle regime. We illustrate the insight gained from these experiments, and discuss how the new experimental data may facilitate verification of theoretical models on a quantitative level.**

***Index Terms*—Non-sequential double ionization, carrier-envelope-phase tagging, strong field physics, near single-cycle laser pulses.**

I. Introduction

NON-SEQUENTIAL double ionization (NSDI) [1], [2] is a strong-field process characterized by the correlated emission of two electrons. This process, which represents an important test case for correlated electron dynamics in strong laser fields, was initially discovered in early experiments where the yield of doubly charged ions was measured as a function of the laser pulse intensity [3], [4]. In these measurements, NSDI manifests as a "knee" in the intensity dependent double-ionization yield curve, which, is not expected in a sequential ionization process, where the first and second ionization steps are assumed to be independent from each other. The impossibility to explain this phenomenon as sequential ionization, led to the name non-sequential ionization.

Manuscript received December 14, 2014; revised April 23, 2015 and May 27, 2015; accepted June 7, 2015.

B. Bergues is with the Max-Planck-Institut für Quantenoptik, Garching D-85748, Germany (e-mail: boris.bergues@mpq.mpg.de).

M. Kübel, N. G. Kling, and C. Burger are with the Ludwig-Maximilians-Universität, Garching D-85748, Germany (e-mail: matthias.kuebel@mpq.mpg.de; nora.kling@physik.lmu.de; christian.burger@mpq.mpg.de).

M. F. Kling is with the Ludwig-Maximilians-Universität, Garching D-85748, Germany, and also with the Max-Planck-Institut für Quantenoptik, Garching D-85748, Germany (e-mail: matthias.kling@mpq.mpg.de).

Color versions of one or more of the figures in this paper are available online at http://ieeexplore.ieee.org.

Digital Object Identifier 10.1109/JSTQE.2015.2443976

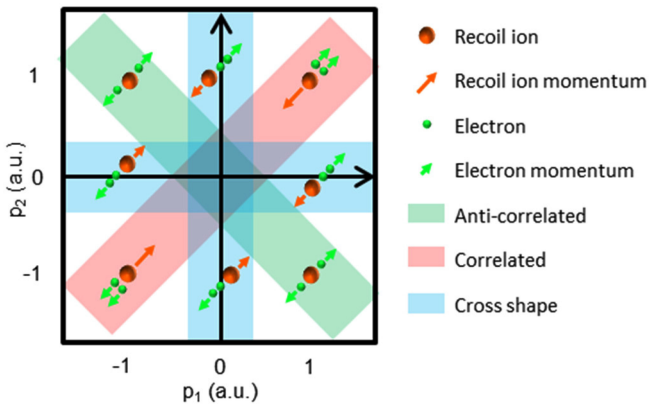

Fig. 1. Two-electron momentum distribution, illustrating the momentum sharing between the two electrons (green spheres) and the doubly charged ion (orange sphere) after double ionization. Events in the red areas in the first and third quadrants correspond to correlated electron emission (i.e., the momentum vectors of the two electrons point to the same direction). Events in the green areas in the second and fourth quadrants correspond to anti-correlated electron emission (i.e., the momentum vectors of the two electrons point to opposing directions). The blue cross- shaped area corresponds to events with totally asymmetric kinetic-energy sharing of the electrons along the laser polarization direction (i.e., one of the two electrons carries most of the kinetic energy). Figure reproduced from Ref. [9]

With the advent of cold target recoil ion momentum spectroscopy (COLTRIMS) [5], [6], NSDI could be investigated in more detail by measuring the momentum distribution of the ions generated in the strong-field ionization process for multiple charge states [7]. Kinematically complete measurements of the double ionization dynamics could finally be obtained by the coincident detection of the two electrons and the doubly charged ion, allowing for the direct observation of the correlated electron momenta [8].

A convenient way to represent the highly differential data, resulting from such coincident measurements, is shown in Fig. 1. In this two-electron momentum distribution, the number of double ionization events is plotted as a function of p_1 and p_2, the momentum components of either electron along a given spatial direction. In the following, p_1 and p_2 will denote the momentum components along the laser polarization direction, which is well suited to capture the essential dynamics of strong field phenomena. Since the two electrons are indistinguishable, the two-electron momentum distributions are symmetrized with respect to the $p_1 = p_2$ main diagonal.

While the two-electron momentum distribution measured at intensities above the knee intensity shows an essentially structure-less distribution, the one recorded in the intensity region below the knee, where NSDI dominates, exhibits a structured two-electron distribution indicating a strong correlation

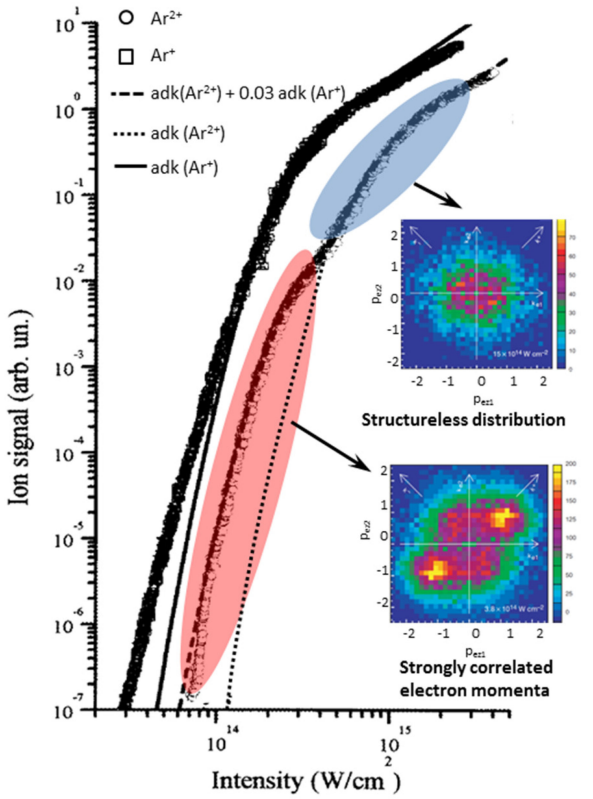

Fig. 2. Yield enhancement and electron correlation in NSDI. Shown is the measured yield of Ar^{+} and Ar^{2+} ions produced by 200 fs pulses of various intensities [22]. The experimental results are fitted with the ADK rate. In the knee region, marked in red, good agreement with the experimental result is obtained by adding a fraction of the ADK rate for Ar^{+} to the Ar^{2+} rate [22]. In the same intensity range, strongly correlated electron momenta are observed in coincidence experiments [8]. At higher intensities above the knee, however, the two-electron momentum distribution assumes a structure less shape. Figure adapted from Refs [22], [8] with permission of IOP publishing, and Nature Publishing Group.

of the electron momenta [8] (see Fig. 2). Since then, NSDI has been investigated in numerous studies, exploring the effect in different target gases and under different regimes regarding, for instance, intensity, wavelength, or polarization of the applied laser field [10]–[21].

It is now widely accepted that the correlated character of the electron emission in NSDI is a consequence of the rescattering process [23], [24], in which a first electron, liberated via tunnel ionization, is strongly accelerated by the laser field and driven back to the parent core where an inelastic collision triggers the ionization of a second electron. In a multi-cycle laser field, such an NSDI process may extend over several laser cycles and result from a complex interplay of multiple recollisions of the electron with the parent ion.

Single-cycle NSDI denotes the limiting case where NSDI is confined to a single optical cycle, such that the ionization of the second electron is triggered by a single recollision [25]. Because it greatly simplifies the calculations, this ideal scenario is often used in the theoretical description of NSDI [17], [20]. The gap between this simple assumption and the more complex reality, however, has impeded quantitative comparison between theory and experiment.

In this sense, the experimental study of single-cycle NSDI is an obvious choice for moving towards quantitative verification of theoretical models. However, its experimental implementation along with the coincident measurement of the electron- and ion-momentum is extremely challenging, which is the reason why all kinematically complete NSDI-experiments, until recently, have been performed in the multi-cycle regime.

Besides the requirement of producing near single-cycle laser pulses [26], single-cycle NSDI experiments also demand controlling or measuring the carrier-envelope phase (CEP) over the entire duration of the experiment. Since the probability for NSDI is orders-of-magnitude lower than that of single ionization, and the rate of detected electrons in a coincidence experiment has to be kept well below one per shot, the acquisition of NSDI events typically last one to several days with a multi-kHz laser system. The control of the CEP over these long time scales has represented one of the major challenges in experimental studies of single-cycle NSDI.

Although first measurements of the CEP-dependence of NSDI in few-cycle pulses have been reported already a decade ago [27], the limited long term CEP-control at that time has restricted these initial studies to the measurement of doubly charged ion momentum distributions and precluded full access to the correlated electron-emission dynamics. It was the combination of single-shot CEP measurement [28] with a reaction microscope (REMI) [6] demonstrated in Refs. [29], [30], that finally allowed for satisfying the requirements for long acquisition times with precise knowledge of the CEP. These advances have resulted in the first measurements of CEP-resolved two-electron momentum distributions from NSDI in the few-cycle [31] and single-cycle [25] regimes.

The dynamics of NSDI of Ar in the extreme limit of a single recollision event [25] strongly contrast with those observed in all experiments using longer pulses. In the present paper, the implementation, results and current interpretation of single-cycle NSDI experiments performed in atomic and molecular targets [9], [25], [30], [32] will be reviewed and discussed. In addition, we highlight which new constraints these highly differential data impose on the development of theoretical models and how they can shed light on the exact mechanisms that govern NSDI.

II. Experimental Methods

The experimental setup for single-cycle NSDI is shown in Fig. 3 and has been described in detail in Refs. [29], [25]. Briefly, linearly polarized laser pulses with a central wavelength around 790 nm are generated at a multi-kHz repetition rate in a chirped-pulse amplification Ti:Sapphire laser system. The pulses with a duration of about 25 fs (FWHM of the intensity envelope) are focused into a hollow-core fiber for spectral broadening and compressed to their near Fourier-limited duration using a chirped-mirror compressor. The laser pulses are split into two beams and individual pairs of fused silica wedges serve to adjust the dispersion and obtain a pulse duration of 4 fs in each beam. The first beam is sent into a single-shot stereo above

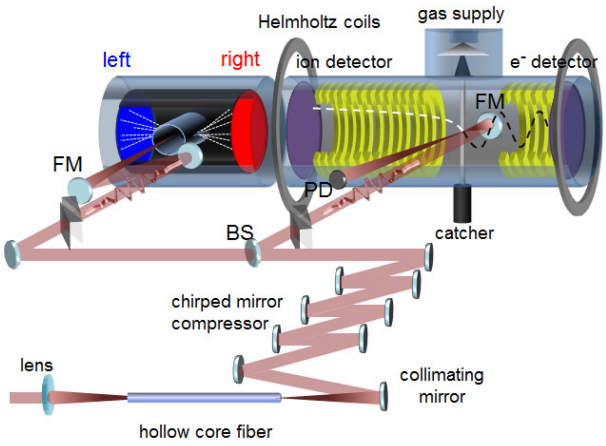

Fig. 3. Schematic of the experimental setup consisting of a single-shot Stereo-ATI phase meter (left chamber) and a REMI spectrometer (right chamber). A beam splitter (BS) and focusing mirrors (FM) direct the laser pulses into both chambers. Each arm is equipped with a pair of fused-silica wedges for compensating residual chirp. In the Stereo-ATI, xenon atoms are ionized near the focus of the horizontally polarized laser beam, and the electrons produced are detected by microchannel-plate (MCP) detectors to the left and to the right, enabling the determination of the CEP for each REMI event. Simultaneously, ions and electrons created in the overlap of the laser focus and a skimmed supersonic jet of the REMI are extracted from the interaction region by a weak electric field (typically 3 $V \cdot cm^{-1}$) and detected by MCPs with delay line anode on the left and right side of the instrument, respectively. The magnetic field produced in two Helmholtz coils facilitates the detection of electrons over a solid angle of 4π. The chamber is efficiently pumped by using a catcher for the jet. The master trigger for the electronics is provided by a fast photodiode (PD). The ion and electron optics are symmetric in reality, and a few electrodes have been removed for visualization of the laser path. Figure reproduced from Ref. [25].

threshold ionization (ATI) phase meter [28] where the CEP of the laser pulse is measured for each and every laser shot up to an unknown constant offset. The second beam is focused into a supersonic argon jet inside a REMI in which the momenta of ions and electrons generated in the laser focus are measured in coincidence. The peak intensity is controlled using an iris at the entrance of the REMI and is estimated from simultaneously measured single-ionization photoelectron spectra of Ar.

III. Single Cycle NSDI of Argon

The CEP-averaged two-electron momentum distribution resulting from single-cycle NSDI of Ar, shown in the center of Fig. 4, exhibits a cross-shaped pattern indicating that the two electrons in single cycle NSDI favor totally asymmetric energy sharing. This result contrasts with all experimental results obtained with longer pulses and suggests that multi-cycle NSDI dynamics may not be understood simply in terms of the sum of independent single-cycle NSDI processes.

The strong impact of the CEP on NSDI can be clearly seen in the CEP-resolved two-electron momentum distributions shown on the ring in Fig. 4, where the angles indicate the measured relative CEPs. Similar, though somewhat smaller, CEP-dependent asymmetries in the two-electron momentum distributions were observed by Camus *et al.*, for NSDI of Ar in the few-cycle regime using a similar experimental set-up.

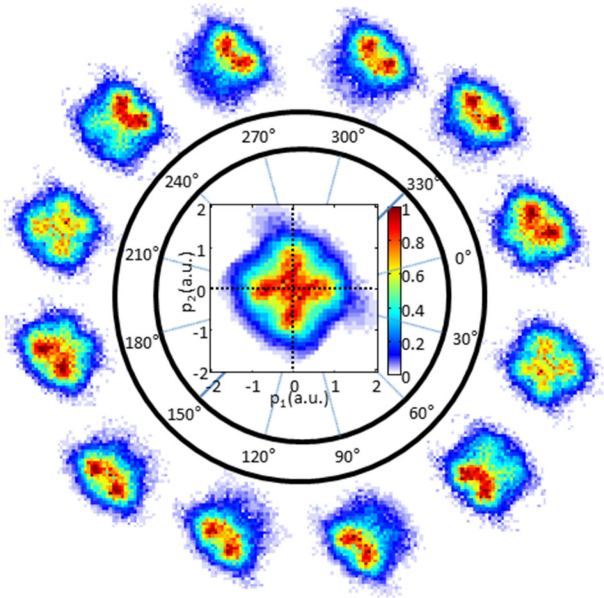

Fig. 4. Two-electron momentum distributions for NSDI of Ar with near-single-cycle laser pulses. The two-electron momentum distribution in the center is averaged over the CEP. The spectra on the outside of the ring are measured for the indicated relative CEP values, and obtained by averaging over a CEP-range of 30°. Each image shows the data using the same momentum scale as the center figure and is normalized to its peak value.

IV. Recollision Excitation With Sub-Cycle Depletion

Essentially two main mechanisms have been invoked earlier to describe recollision induced NSDI [2]. In the first one, the direct electron impact ionization or (e,2e)-process, the first electron is liberated via tunnel ionization and the second electron is ionized via direct impact ionization upon recollision. In the second one, the recollision excitation and subsequent tunneling (RESI) mechanism, the recolliding electron excites the singly-charged ion, which is further ionized by the laser field, e.g., via tunnel ionization after a time delay τ.

In order to gain a deeper understanding of the experimental results shown in Fig. 4, both mechanisms have been implemented in a simple one-dimensional semi-classical model. The best agreement with the data was obtained assuming the "recollisional excitation with sub-cycle depletion" scenario described in Ref. [25].

The essence of this model is as follows: after tunnel ionization, the first electron emerges at the tunnel exit with zero initial momentum. Its continuum evolution in the presence of the electric field of the laser is described classically, neglecting Coulomb interactions. The electron-core interaction and the excitation upon recollision are modeled as point-like events in time, which take place at the moment where the electron crosses the position of the parent ion. For the recollision excitation step, only the lowest excited state of Ar^+ (with an excitation energy $E_{exc} = 13.5$ eV) is considered and populated by electrons recolliding with a kinetic energy $E_r > 13.5$ eV. After the inelastic recollision, the recolliding electron is further propagated in the laser field with an initial momentum $p = \sqrt{\frac{2(E_r - E_{exc})}{m}}\cos(\beta)$,

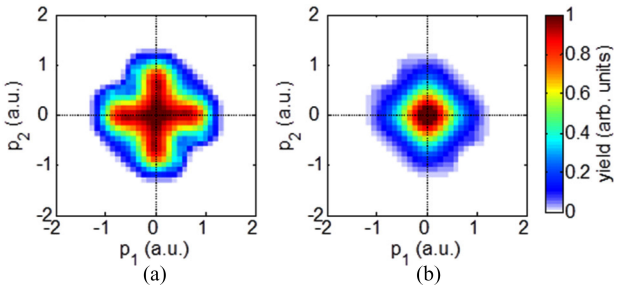

Fig. 5. CEP-averaged two-electron momentum distributions calculated for NSDI of Ar by a 3.8 fs pulse with a center wavelength around 750 nm, and a peak intensity of 2.9×10^{14} W/cm^2. In (a) sub-cycle depletion is considered, in (b) sub-cycle depletion is ignored.

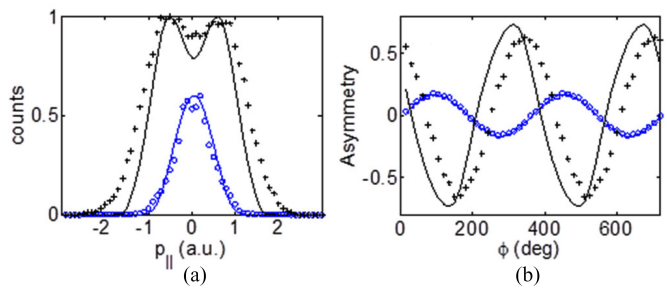

Fig. 6. Quantitative comparison between experiment and theory. (a) The recorded momentum spectra along the polarization axis for Ar^+ (blue circles) and Ar^{2+} (black crosses) are compared to their calculated counter parts (solid blue and black lines for Ar^+ and Ar^{2+}, respectively). For visual convenience, the Ar^+ spectra in (a) are normalized to 0.6. (b) CEP-dependent asymmetries in the directional yields of Ar^+ (blue circles) and Ar^{2+} (black crosses). Because the CEP is only measured up to an unknown offset, the experimental data were shifted such that the phase of the Ar^+ CEP-dependent asymmetry oscillation agrees with the calculated curve. The phase of the calculated Ar^{2+} asymmetry oscillation exhibits a discrepancy of 40° with respect to the measured Ar^{2+} asymmetry.

where β denotes the angle between the electron momentum just before and just after the recollision. With the introduction of the free parameter β scattering into another dimension can be account for in the one dimensional model. The best agreement between theory and experiment is found for $\beta = 20$. For the second ionization step, the excited state is depleted by the laser field via tunnel ionization. In contrast to conventional RESI models [11], [33], however, we do not make the ad-hoc assumption that the second electron is released only at the next peak of the laser cycle and consider depletion of the excited state population on a sub-cycle time scale. For both ionization steps we make use of the ionization rates of Tong and Lin [34] that remain accurate in the barrier-suppression regime. Focal volume averaging is taken into account by assuming a Gaussian intensity profile in the interaction region.

The key role of sub-cycle depletion in the formation of the cross pattern is demonstrated in Fig. 5, where recollisional excitation with sub-cycle depletion (see Fig. 5(a)) is compared to the case where depletion is ignored, i.e., to the case where the electron is simply released at the next peak of the laser cycle (see Fig. 5(b)). It can be seen that the measured CEP-averaged two-electron momentum distribution shown in Fig. 4 is well described only when sub-cycle depletion is taken into account.

V. Quantitative Comparison With Theory

In order to fit the measured data with a theoretical model, it is important to consider all the information provided by the measurement. The single ionization events recorded in the same measurement, for instance, provide additional constraints that need to be accounted for, in a consistent fitting procedure. In the fitting procedure used in Ref. [25], the width of the Ar^+ momentum spectrum is used to determine the instantaneous peak intensity of the laser pulse with 2.9×10^{14} W/cm^2 with a (model dependent) accuracy of 20%.

For an objective and more quantitative comparison of the measured data with the theoretical fit, it is essential to go beyond simple comparison of color map images and consider different projections of the multi-dimensional data. An example of such projections is shown in Fig. 6(a), where the measured CEP-averaged momentum distributions of Ar^+ and Ar^{2+} are compared to the calculated ones. Apart from the slightly too narrow wings, the Ar^{2+} spectrum is fairly well reproduced by the theoretical fit.

Another projected quantity, which is useful to quantify CEP effects is the asymmetry parameter $A = (N^+ - N^-)/(N^+ + N^-)$, where N^+ and N^- are the number of ions with positive and negative momentum along the polarization axis, respectively.

The measured and calculated CEP-dependent asymmetries of the Ar^+ and Ar^{2+} yields are shown in Fig. 6(b). Since the CEP of the laser pulses in the interaction region is known only up to a common offset value, this offset value is chosen so that the measured Ar^+ asymmetry curve is in phase with the calculated one. While the phase of the measured Ar^+ asymmetry is thus of no significance, both the amplitude and shape of the calculated Ar^+ asymmetry curve can be compared to the experimental data and perfect agreement is found for a pulse duration of 3.8 fs (FWHM in intensity), which is consistent with the result of the experimental pulse duration diagnostics.

In contrast to the phase of the Ar^+ asymmetry, the relative phase shift $\Delta\varphi$ between the Ar^+ and Ar^{2+} CEP-dependent asymmetries is a well-defined experimental observable that imposes new constraints to theoretical models. While the amplitudes of the calculated and measured Ar^{2+} asymmetry curves shown in Fig. 6(b) are in fairly good agreement, the phase shift $\Delta\phi$ between the two curves is not correctly reproduced. This discrepancy of about 40° seems to persist when varying the intensity [35]. Despite the small discrepancies mentioned above, it is quite remarkable how accurately the experimental data can be fitted by such a simple model.

VI. Model Interpretation

It is instructive to use the results of this simple model to interpret the experimental results. In Fig. 7, we investigate two special cases corresponding to CEP values leading to zero and maximum Ar^{2+} asymmetry, respectively. For a CEP maximizing the asymmetry (upper panels in Fig. 7), the NSDI process is triggered by a single recollision. In this case the excited Ar^+

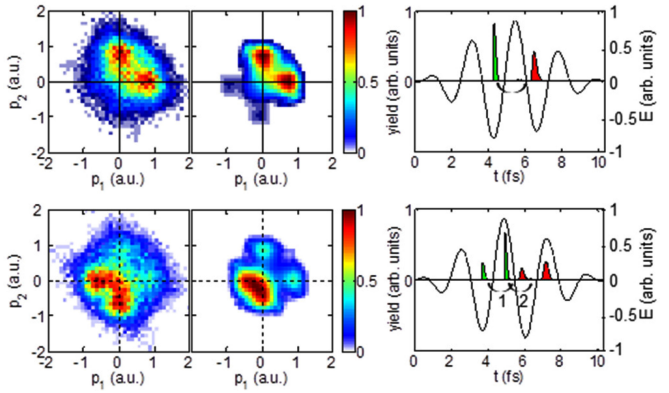

Fig. 7. Timing of the first and second ionization step in single-cycle NSDI of Ar. Shown are the measured (left panels) and calculated (middle panels) two-electron momentum distributions for CEPs corresponding to maximum (upper panels), and zero (lower panels) asymmetry. Furthermore, the laser electric field and the calculated ionization rates for the first (green) and second (red) electron contributing to NSDI are displayed in the right panels. The calculations reveal that after recollision, indicated by the black arrows, the emission of the second electron occurs before the electric field maximum is reached.

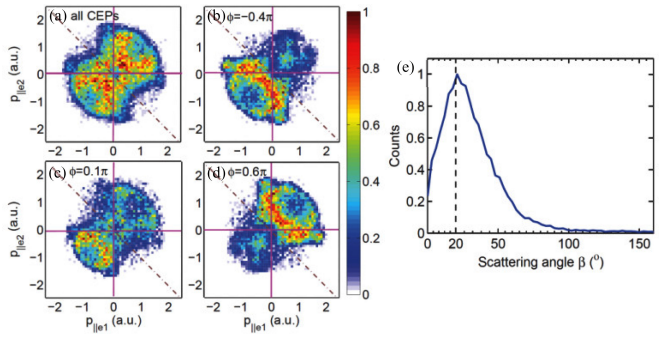

Fig. 8. Calculated two-electron momentum distributions for single-cycle NSDI of Ar by 3.64 fs pulses with a central wavelength around 750 nm and a peak intensity of 3×10^{14} W/cm^2, averaged over the CEP φ (a), and for the CEP-values leading to (b and d) maximum and (c) zero asymmetry in the emission direction of the doubly charged ions. The results were obtained with a classical ensemble model [40]. (e) Distribution of the scattering angle β for $\phi = 0.6\ \pi$. Figure reproduced from Ref. [40] with permission of The Optical Society.

state is depleted 230 as before the field maximum. For a CEP where the asymmetry is near zero, in contrast, two recollision processes contribute to NSDI. As explained in detail in Ref. [25], the first and second NSDI events can be experimentally distinguished since they populate the upper-right half and lower-left half of the two electron momentum distribution, respectively.

According to the model, it is depletion of the excited Ar^+ state before the maximum of a laser cycle that causes the second electron to acquire large momentum values (while the choice of the parameter β confines the final momentum of the first electron to small values around zero). This interpretation contrasts with the common idea that the large momentum in RESI is acquired by the first electron, while the second electron is released at a maximum of the electric field [36]. Both scenarios can give rise to a cross-shape in the CEP-averaged two-electron momentum distribution.

VII. Alternative Models and Interpretations

The good agreement between the theoretical fit and the measured data also raises the question of possible over fitting. In the procedure followed in Ref. [25], the Ar^+ spectrum and asymmetry are used to fix the peak intensity and pulse duration, respectively, within the range of experimental uncertainties. The requirement to reproduce a cross shaped two-electron momentum distribution fixes the value of the free parameter β. Hence, no more parameters are used in the simple model to match the CEP-resolved Ar^{2+} spectrum, and its projections: the CEP averaged spectrum and the asymmetry. These two observables are thus a measure for the accuracy of the model.

The assumed Dirac delta distribution for β and the restriction to the lowest excited state of Ar^+ are very rough simplifications of reality, where the scattering angles are expected to be distributed over a finite angular range, and higher excited states of Ar^+ may also be populated. The good agreement of the simulation results with the data (see Fig. 7) might indicate, however, that the lowest excited state of Ar^+ and the value chosen for β are dominating in the NSDI process.

Relaxing the requirement of a single β value and allowing for contributions of higher-lying excited states of Ar^+, could easily remove the discrepancy between measurements and simulations. Since neither the electron impact excitation cross sections nor the scattering angles are known, fitting distributions for these two quantities as free parameters would, however, result in a clear case of over fitting.

More sophisticated models that are efficient enough to allow calculations over a broad range of experimental and/or model parameters are thus needed to refine our understanding of NSDI. Importantly, the accuracy of such models should be validated by a quantitative comparison with all the projections of the measured multi-dimensional data.

A number of different approaches have been used for the theoretical description of NSDI [1]. A promising approach for the treatment of laser-driven recollision processes is the quantitative rescattering theory [37] (QRS), given the relevant electron-impact cross-sections are known. In Ref. [38], Chen *et al.* have used QRS to model NSDI of Ar [39] in few-cycle laser fields and found good agreement with the measured CEP-dependent ion spectra from Ref. [29]. However, a similar good agreement of the simulations with the measured two-electron momentum distributions from Ref. [25] has not yet been demonstrated. More recently, the experimental data have been simulated by Huang *et al*. [40] using classical ensemble calculations [41], [42].

The results of the simulations are shown in Fig. 8. Apart from the qualitative agreement of the calculated two-electron momentum distributions with the measured data (see Figs. 4 and 7), an interesting outcome of this study is the calculated distribution of scattering angles β that shows a maximum at 20°, which coincides with the value that best fits the experimental data in the simple model of Ref. [25]. Since neither the CEP-dependent Ar^+ asymmetry nor the CEP-averaged Ar^+ and Ar^{2+} spectra are provided in Ref. [40], a more quantitative comparison of the calculation results (in particular the predicted

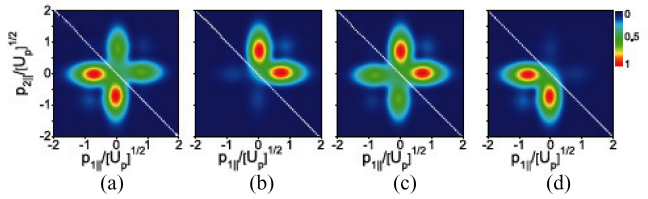

Fig. 9. Two-electron spectra for single-cycle NSDI of Ar calculated by Faria and coworkers [43] for a peak intensity of 1.5×10^{14} W/cm^2. The electron momenta $p_{1||}$ and $p_{2||}$ are plotted in atomic units of $\sqrt{\mathbf{Up}}$, where U_p is the ponderomotive energy. Figure reproduced from Ref. [43] with permission of The American Physical Society.

phase shift between the Ar^+ and Ar^{2+} asymmetry curves) with the experimental data is not possible.

Strong field approximation based quantum mechanical computations of the RESI process were carried out by Faria *et al.* [43]. The two-electron momentum distributions calculated for single cycle NSDI of Ar at a peak intensity of 1.5×10^{14} W/cm^2 are shown in Fig. 9. Their shapes are in qualitative agreement with the measured ones.

A significant advantage of this approach is that it is truely three dimensional and naturally includes quantum interference effects. In a previous study [36] it was found that the shape of the two electron momentum distribution in RESI is essentially determined by the excited state involved in the process. In Ref. [43], for instance, the cross shape results from the excitation from a 3p to a 4s state.

The results of [43] lead to the interpretation that it is the first (i.e., the recolliding) electron that acquires the large momentum values forming the cross and not the second electron, which contrasts with the conclusions drawn from of the simple model presented in Section IV and in Ref. [25]. Although depletion was only accounted for partially in Ref. [43], only a minor role was ascribed to depletion in the formation of the cross. Assessing the validity of the quantum model of Ref. [43] clearly requires a more detailed comparison of the quantum simulations with the experimental data, in particular with the measured data shown in Fig. 6.

VIII. Continuative Experimental Single-Cycle NSDI Studies

Since the initial study [25] discussed above, further experimental studies addressing single-cycle NSDI of nitrogen [32] and the transition from single- to multi-cycle NSDI [9], have provided additional constraints for theoretical models.

A. Argon Versus Nitrogen

Because the first and second ionization potentials of Ar and N_2 are similar, NSDI in both gases can be observed under the same experimental conditions. This allows for designing an experiment where NSDI of both targets can be measured simultaneously, i.e., for the exact same laser parameters, and makes N_2 and Ar ideal candidates for quantitative comparison of single-cycle NSDI of two different targets. Because of the similarity of the ionization potentials, the two targets are

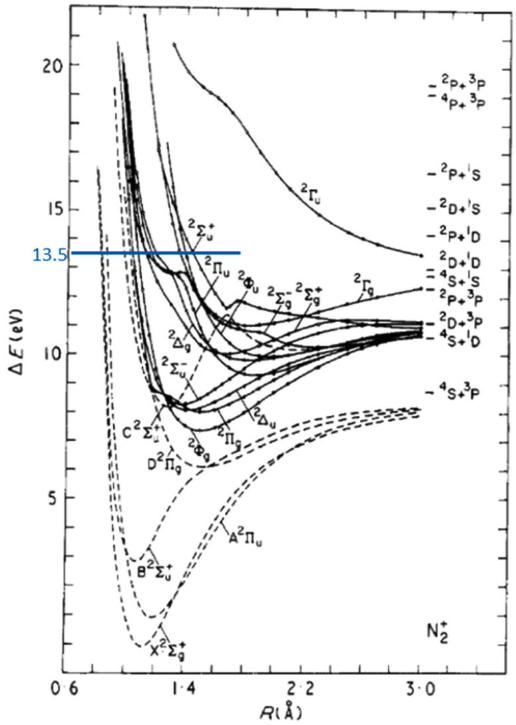

Fig. 10. Comparison of the lowest energy levels in N_2^+ with the lowest excited state of Ar^+ (blue line) that lies 13.5 eV above the Ar^+ ground state at $\Delta E = 0$. Figure reproduced from Ref. [45] with permission of IOP publishing.

known to exhibit similar ionization behavior [44]. Despite these similarities, however, Ar^+ and N_2^+ have significantly different excited-state spectra. This is illustrated in Fig. 10, where it can be seen, in particular, that the N_2^+ ion has several excited states with energies ranging far below the first excited state of Ar^+ at 13.5 eV.

This fact has an important consequence for models involving the excited state spectrum of the singly charged ions. In particular, it might be questioned whether the assumptions of Ref. [25] regarding the involved excited states, can withstand the experimental test.

The experimental results of Ref. [32] where a direct comparison of single-cycle NSDI of Ar and N_2 was performed are shown in Figs. 11 and 12. As can be seen in Fig. 11, the CEP-resolved two-electron momentum distributions from N_2 are qualitatively similar to the ones of Ar. The same is true for the CEP-averaged momentum distributions that exhibit the same cross shaped structure for both targets.

A closer inspection of the CEP-resolved Ar^{2+} and N_2^{2+} spectra in Fig. 12(a) and (b), however, reveals small but significant differences between the two targets. In order to quantify these differences we consider the projections shown in Fig. 12(c) and (d). The first difference concerns the dip at zero momentum in the CEP-averaged N_2^{2+}-spectrum, which is shallower than the corresponding Ar^{2+}-spectrum. The second difference concerns the amplitude of the CEP-dependent N_2^{2+} asymmetry, which is slightly smaller than that of Ar^{2+}. For the singly-charged ions of the two species, in contrast, the CEP-averaged spectra and

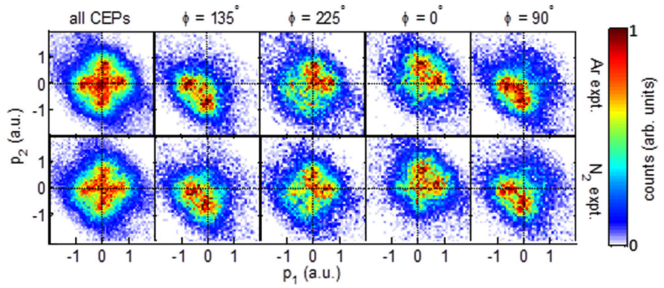

Fig. 11. Experimental two-electron momentum distributions showing the correlated momenta along the laser polarization axis of the first (p_1) and second (p_2) electrons emitted from Ar^{2+} (top row) or N_2^{2+} (bottom row). The CEP-averaged results are displayed in the far left column. In the second through fifth columns, the correlation spectra are shown for CEP values of -45 °, 45°, 180°, and 270°, respectively. The signal in each image is averaged over a CEP range of ± 22.5° and normalized to its maximum value. The undetermined CEP offset in the experimental data was chosen such that measured and calculated doubly charged ion spectra oscillate in phase. Invariance under the symmetry transformation $(p, \varphi) \rightarrow (-p, \varphi + \pi)$ and the symmetry with respect to the $p_2 = p_1$ diagonal were used to symmetrize the measured distributions.

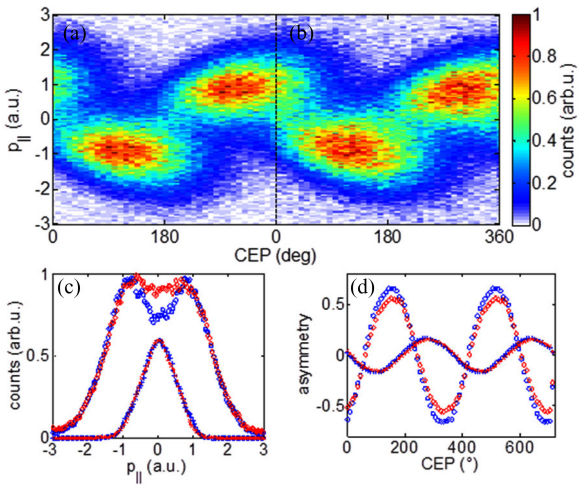

Fig. 12. CEP- dependence of the doubly-charged-ion momentum distributions for single-cycle NSDI of (a) Ar and (b) N_2, recorded simultaneously. (c) CEP-averaged ion momentum distributions for Ar^+ (blue crosses), N_2^+ (red crosses), Ar^{2+} (blue circles), N_2^{2+} (red circles). For visual convenience, the Ar^+ and N_2^+ spectra in (c) are normalized to 0.6. (d) The asymmetry parameter for all ion species using the same color coding.

CEP-dependent asymmetry curves are essentially identical within the experimental resolution.

It was shown in Ref. [32] that the differences between the two species may be understood in terms of recollision excitation with sub-cycle depletion, if additional NSDI-contributions from lower lying excited states of N_2^+ are considered. Here, lower lying states refer to excited states with excitation energies below that of the first excited state of Ar^+. The impact of these states on recollision excitation is illustrated in Fig. 13. Since the probability that the second electron is tunnel ionized from an excited sate rapidly decreases with decreasing excitation energy, lower excited states are depleted closer to an extremum of the electric field. When the excitation energy is decreased the two-electron momentum distribution is thus confined to a smaller and

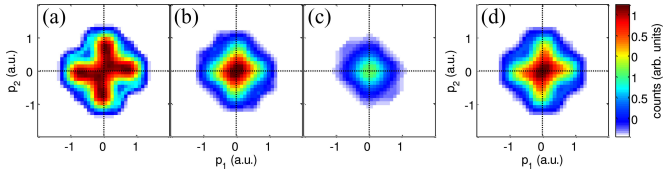

Fig. 13. Dependence of the calculated two-electron momentum distributions on the excitation energy. (a) $E_{exc} = 13.5$ eV, (b) $E_{exc} = 11.5$ eV, (c) $E_{\rm exc} = 13.5$ eV, (d) the sum of (a–c).

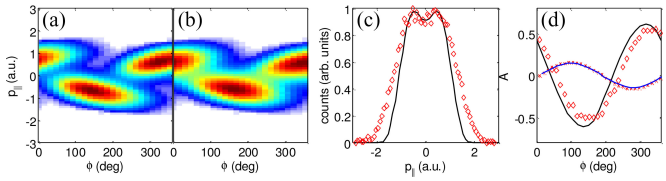

Fig. 14. Results of the adapted calculations for NSDI of N_2 where two lower lying excited states with $I_P = 16$ eV and $I_P = 18$ eV were considered in addition to the lowest excited state of Ar with $I_P = 14$ eV. (a) The CEP-resolved Ar^{2+} momentum spectrum using only the state with $I_P = 14$ eV, (b) the ion momentum spectrum, considering all three states. (c) Measured N_2^{2+} momentum distribution, averaged over CEP (red circles) and the calculated spectrum using the adapted calculations. (d) same for the asymmetry parameter for N_2^{2+}, shown along with experimental and theoretical results for single ionization of N_2.

smaller region around the origin, as shown in Fig. 13(a)–(c). The rapidly decreasing tunneling probability also provides an explanation for the overall limited impact of lower lying states on the two-electron momentum distribution (see Fig. 13(d)).

As can be seen in Fig. 14, a contribution of lower lying states in N_2^+ may yield an explanation for the differences observed in the single-cycle NSDI of the two species. The results of the above example calculation show that the recollision excitation with sub-cycle depletion model is still consistent with the experimental data for single-cycle NSDI of N_2^+. However, these results cannot validate the assumptions of the model since the choice of the lower-lying excited states and their relative contributions remains arbitrary without knowledge of the electron impact excitation cross sections.

B. Transition to the Multi-Cycle Regime

In view of the significant differences observed between single-cycle- and multi-cycle NSDI, studying the transition of its dynamics from the near-single to the multi-cycle regime is certainly one of the keys to gain a deeper understanding of the process. For Ar the transition was investigated experimentally in [9], where the duration of the near transform-limited laser pulses were varied in a range from 4 to 30 fs, for a fixed peak intensity. The two-electron momentum distributions recorded in this study are shown in Fig. 15. It can be seen that the major changes occurs in the few-cycle regime between 4 and 8 fs where the cross-shaped two-electron momentum distribution collapse to a rather structure less distribution. As shown in detail in Ref. [9], this transition to longer pulses is further accompanied by a strong increase in the fraction of anti-correlated to correlated electrons. It was also confirmed there that increasing

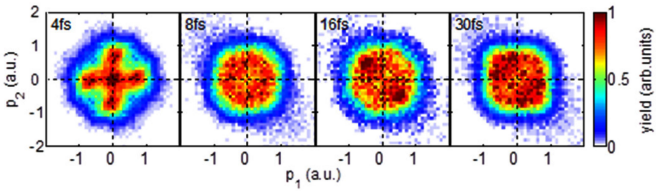

Fig. 15. CEP-averaged two-electron momentum distribution for NSDI of Ar for pulse durations from the single to the many-cycle regime, as indicated in the figure. The focal intensity, estimated from the $10U_P$ cut-offs in the simultaneously recorded Ar^+ photoelectron spectra, is kept constant at around 10^{14} W/cm^2 within 15% accuracy.

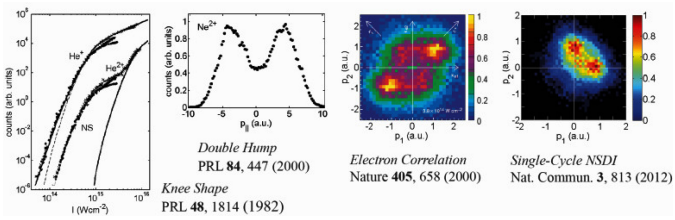

Fig. 16. Milestones in the experimental research of strong-field non-sequential double ionization. Shown are the key signatures of NSDI with the publications in which they appeared. Figure adapted from Refs. [47], [7], [8], and [25] with permission from the American Physical Society and Nature Publishing Group.

the laser intensity enhances the positively correlated electron signal, which is consistent with the results of Ref. [8] recorded at a much higher intensity.

Earlier theoretical studies following the classical-ensemble approach [41] have pointed out the role of multiple recollisions in the production of anti-correlated electrons [19]. Because of the large number of additional ad-hoc assumptions it would require, an extension of the simple model of Ref. [25] to include multiple recollisions is not meaningful.

Classical ensemble calculations may be a promising alternative, since multiple recollisions are naturally included in this approach, and qualitative agreement with experimental results has already been demonstrated in the limit of single cycle NSDI [40]. Moreover, such classical calculations can describe the formation of doubly excited states. In Refs. [31] and [46], the NSDI dynamics of Ar by few and many-cycle laser pulses, respectively, could be explained by the formation and decay of a doubly excited state. The population of such states in strong laser fields may represent another important pathway leading to NSDI.

IX. Conclusion

As illustrated in Fig. 16, the experimental implementation of single-cycle NSDI represents a new milestone in the experimental investigation of correlated electron dynamics in strong laser fields. Because of the lower level of complexity required for their modeling, kinematically complete single-cycle NSDI experiments should stimulate the development of theoretical models, and facilitate their quantitative verification.

While the simple model for recollision-excitation with subcycle depletion performs fairly well in describing single cycle NSDI of Ar, its predictive power is limited by the need for an ad-hoc assumptions regarding the value of the scattering angle β and the choice of the intermediate excited states. From the theoretical side, more sophisticated but still efficient ab-initio calculations are thus desirable. A particular challenge for theory will be the quantitative description of the transition from single-cycle to multi-cycle NSDI with a single set of parameters. To our knowledge, this transition has not been reproduced in simulations so far, and still remains to be understood.

Acknowledgment

The authors would like to thank fruitful discussions with C. F. de Morisson Faria and T. Shaaran, and collaborators that have contributed to the results contained in this review, in particular, F. Krausz, U. Kleineberg, G.G. Paulus, I. Ben-Itzhak, T. Pfeifer, R. Moshammer, and J. Ullrich for their support and for making specialized equipment available to us. They also thank the support from the Max Planck Society, from the DFG via the Cluster of Excellence: Munich Center for Advanced Photonics, and an LMU Excellence Grant, and from the EU by the ERC Grant ATTOCO. B. Bergues would like to thank additional support from L. Veisz.

References

[1] C. F. de Morisson Faria and X. Liu, "Electron–electron correlation in strong laser fields," *J. Mod. Opt.*, vol. 58, no. 13, pp. 1076–1131, Jul. 2011.
[2] W. Becker, X. Liu, P. J. Ho, and J. H. Eberly, "Theories of photoelectron correlation in laser-driven multiple atomic ionization," *Rev. Mod. Phys.*, vol. 84, no. 3, pp. 1011–1043, Jul. 2012.
[3] I. Aleksakhin, I. Zapesochnyi, and V. Suran, "Double multiphoton ionization of strontium atom," *JETP*, vol. 26, no. 1, pp. 11–12, 1977.
[4] A. L'Huillier, L. A. Lompre, G. Mainfray, and C. Manus, "Multiply charged ions formed by multiphoton absorption processes in the continuum," *Phys. Rev. Lett.*, vol. 48, no. 26, pp. 1814–1818, 1982.
[5] R. Dörner *et al.*, "Cold target recoil ion momentum spectroscopy: A 'momentum microscope' to view atomic collision dynamics," *Phys. Rep.*, vol. 330, pp. 95–192, 2000.
[6] J. Ullrich *et al.*, "Recoil-ion and electron momentum spectroscopy: Reaction-microscopes," *Rep. Prog. Phys.*, vol. 66, pp. 1463–1545, 2003.
[7] R. Moshammer *et al.*, "Momentum distributions of ne(n+) ions created by an intense ultrashort laser pulse," *Phys. Rev. Lett.*, vol. 84, no. 3, pp. 447–450, Jan. 2000.
[8] T. Weber *et al.*, "Correlated electron emission in multiphoton double ionization," *Nature*, vol. 405, no. 6787, pp. 658–661, Jun. 2000.
[9] M. Kübel *et al.*, "Non-sequential double ionization of Ar: from the single- to the many-cycle regime," *New J. Phys.*, vol. 16, no. 3, p. 033008, Mar. 2014.
[10] C. Guo and G. Gibson, "Ellipticity effects on single and double ionization of diatomic molecules in strong laser fields," *Phys. Rev. A*, vol. 63, no. 4, pp. 040701-1–040701-4, Mar. 2001.
[11] B. Feuerstein *et al.*, "Separation of recollision mechanisms in nonsequential strong field double ionization of Ar: The role of excitation tunneling," *Phys. Rev. Lett.*, vol. 87, no. 4, pp. 043003-1–043003-1, Jul. 2001.
[12] E. Eremina *et al.*, "Influence of molecular structure on double ionization of N2 and O2 by high intensity ultrashort laser pulses," *Phys. Rev. Lett.*, vol. 92, no. 17, pp. 173001-1–173001-4, Apr. 2004.
[13] M. Weckenbrock *et al.*, "Fully differential rates for femtosecond multiphoton double ionization of neon," *Phys. Rev. Lett.*, vol. 92, no. 21, pp. 213002-1–213002-4, May 2004.
[14] A. Rudenko *et al.*, "Correlated multielectron dynamics in ultrafast laser pulse interactions with atoms," *Phys. Rev. Lett.*, vol. 93, no. 25, pp. 253001-1–253001-4, Dec. 2004.
[15] D. Zeidler *et al.*, "Controlling attosecond double ionization dynamics via molecular alignment," *Phys. Rev. Lett.*, vol. 95, no. 20, pp. 203003-1–203003-4, Nov. 2005.

[16] A. Rudenko *et al.*, "Correlated two-electron momentum spectra for strong-field nonsequential double ionization of he at 800 nm," *Phys. Rev. Lett.*, vol. 99, no. 26, pp. 263003-1–263003-4, Dec. 2007.
[17] A. Staudte *et al.*, "Binary and recoil collisions in strong field double ionization of helium," *Phys. Rev. Lett.*, vol. 99, no. 26, pp. 263002-1–263002-4, Dec. 2007.
[18] O. Herrwerth *et al.*, "Wavelength dependence of sub-laser-cycle few-electron dynamics in strong-field multiple ionization," *New J. Phys.*, vol. 10, no. 2, pp. 025007-1–025007-16, Feb. 2008.
[19] Y. Liu *et al.*, "Strong-field double ionization of Ar below the recollision threshold," *Phys. Rev. Lett.*, vol. 101, no. 5, pp. 053001-1–053001-4, Jul. 2008.
[20] A. Emmanouilidou and A. Staudte, "Intensity dependence of strong-field double-ionization mechanisms: From field-assisted recollision ionization to recollision-assisted field ionization," *Phys. Rev. A*, vol. 80, no. 5, pp. 053415-1–053415-7, Nov. 2009.
[21] L. Zhang *et al.*, "Subcycle control of electron-electron correlation in double ionization," *Phys. Rev. Lett.*, vol. 112, no. 19, pp. 193002-1–193002-5, May 2014.
[22] S. Larochelle, A. Telebpour, and S. L. Chin, "Non-sequential multiple ionization of rare gas atoms in a Ti: Sapphire laser field," *J. Phys. B, At. Mol. Opt. Phys*, vol. 31, p. 1201, 1998.
[23] J. Krause, K. Schafer, and K. Kulander, "High-order harmonic generation from atoms and ions in the high intensity regime," *Phys. Rev. Lett.*, vol. 68, no. 24, pp. 3535–3538, 1992.
[24] P. B. Corkum, "Plasma perspective on strong field multiphoton ionization," *Phys. Rev. Lett.*, vol. 71, no. 13, pp. 1994–1997, 1993.
[25] B. Bergues *et al.*, "Attosecond tracing of correlated electron-emission in non-sequential double ionization," *Nature Commun.*, vol. 3, pp. 813-1–813-6, 2012.
[26] F. Krausz and M. Ivanov, "Attosecond physics," *Rev. Mod. Phys.*, vol. 81, no. 1, pp. 163–234, Feb. 2009.
[27] X. Liu *et al.*, "Nonsequential double ionization at the single-optical-cycle limit," *Phys. Rev. Lett.*, vol. 93, no. 26, pp. 263001-1–263001-4, Dec. 2004.
[28] T. Wittmann *et al.*, "Single-shot carrier–envelope phase measurement of few-cycle laser pulses," *Nature Phys.*, vol. 5, no. 5, pp. 357–362, Apr. 2009.
[29] N. G. Johnson *et al.*, "Single-shot carrier-envelope-phase-tagged ion-momentum imaging of nonsequential double ionization of argon in intense 4-fs laser fields," *Phys. Rev. A, At. Mol. Opt. Phys.*, vol. 83, pp. 013412-1–013412-5, 2011.
[30] M. Kübel *et al.*, "Carrier-envelope-phase tagging in measurements with long acquisition times," *New J. Phys.*, vol. 14, no. 9, pp. 093027-1–093027-11, Sep. 2012.
[31] N. Camus *et al.*, "Attosecond correlated dynamics of two electrons passing through a transition state," *Phys. Rev. Lett.*, vol. 108, no. 7, pp. 073003-1–073003-5, Feb. 2012.
[32] M. Kübel *et al.*, "Nonsequential double ionization of N_2 in a near-single-cycle laser pulse," *Phys. Rev. A*, vol. 88, no. 2, pp. 023418-1–023418-6, Aug. 2013.
[33] R. Kopold, W. Becker, H. Rottke, and W. Sandner, "Routes to nonsequential double ionization," *Phys. Rev. Lett.*, vol. 85, no. 18, pp. 3781–3784, Oct. 2000.
[34] X. M. Tong and C. D. Lin, "Empirical formula for static field ionization rates of atoms and molecules by lasers in the barrier-suppression regime," *J. Phys. B, At. Mol. Opt. Phys.*, vol. 38, no. 15, pp. 2593–2600, Aug. 2005.
[35] M. Kübel, "Single-cycle non-sequential double ionization," Dept. Physics, Ludwig-Maximilians Univ., Munich, Germany, 2014.
[36] T. Shaaran, M. T. Nygren, and C. Figueira de Morisson Faria, "Laser-induced nonsequential double ionization at and above the recollision-excitation-tunneling threshold," *Phys. Rev. A*, vol. 81, no. 6, pp. 063413-1–063413-14, Jun. 2010.
[37] T. Morishita, A.-T. Le, Z. Chen, and C. D. Lin, "Accurate Retrieval of structural information from laser-induced photoelectron and high-order harmonic spectra by few-cycle laser pulses," *Phys. Rev. Lett.*, vol. 100, no. 1, pp. 013903-1–013903-4, Jan. 2008.
[38] Z. Chen, Y. Liang, D. H. Madison, and C. D. Lin, "Strong-field nonsequential double ionization of Ar and Ne," *Phys. Rev. A*, vol. 84, no. 2, pp. 023414-1–023414-9, Aug. 2011.
[39] S. Micheau, Z. Chen, A.-T. Le, and C. Lin, "Quantitative rescattering theory for nonsequential double ionization of atoms by intense laser pulses," *Phys. Rev. A*, vol. 79, no. 1, pp. 013417-1–013417-6, Jan. 2009.
[40] C. Huang, Y. Zhou, Q. Zhang, and P. Lu, "Contribution of recollision ionization to the cross-shaped structure in nonsequential double ionization," *Opt. Exp.*, vol. 21, no. 9, pp. 11382–11390, May 2013.
[41] R. Panfili and J. H. Eberly, "Comparing classical and quantum dynamics of strong-field double ionization," vol. 8, no. 7, pp. 431–435, 2001.
[42] S. Haan, L. Breen, A. Karim, and J. Eberly, "Variable time lag and backward ejection in full-dimensional analysis of strong-field double ionization," *Phys. Rev. Lett.*, vol. 97, no. 10, pp. 103008-1–103008-4, Sep. 2006.
[43] C. Faria, T. Shaaran, and M. Nygren, "Time-delayed nonsequential double ionization with few-cycle laser pulses: Importance of the carrier-envelope phase," *Phys. Rev. A*, vol. 86, pp. 053405-1–053405-12, 2012.
[44] C. Guo, M. Li, J. Nibarger, and G. Gibson, "Single and double ionization of diatomic molecules in strong laser fields," *Phys. Rev. A*, vol. 58, no. 6, pp. R4271–R4274, Dec. 1998.
[45] D. C. Cartwright and T. Dunning, "New electronic states of N_2^+," *J. Phys. B, At. Mol. Opt. Phys.*, vol. 8, pp. L100–L104, 1975.
[46] Y. Liu *et al.*, "Strong-field double ionization through sequential release from double excitation with subsequent coulomb scattering," *Phys. Rev. Lett.*, vol. 112, no. 1, pp. 013003-1–013003-5, Jan. 2014.
[47] B. Walker, B. Sheehy, and L. DiMauro, "Precision measurement of strong field double ionization of helium," *Phys. Rev. Lett.*, vol. 73, no. 9, pp. 1227–1230, 1994.

Boris Bergues was born in Grenoble, France. He received the physics Diploma in theoretical quantum dynamics in 2003 from the University of Freiburg, Freiburg im Breisgau, Germany, where he also completed his Ph.D. on strong-field photo-detachment of negative ions in 2008.

Since 2008, he has been working in the Laboratory of Attosecond Physics at the Max-Planck Institute of Quantum Optics. His research interests include strong-field and attosecond Physics with emphasis on multi-particle dynamics in atomic and molecular systems, and the generation of intense isolated attosecond pulses for the study of nonlinear light-matter interactions in the XUV.

Matthias Kübel received his Diploma degree in physics from the Friedrich-Schiller University of Jena, Germany, in 2010 and received the Ph.D. degree from the Ludwig-Maximilians University of Munich, Germany, in 2014. Since 2014, he has been a Research Assistant at the Ludwig-Maximilians University Munich. He is an author of more than 30 articles. His research interests include ionization and dissociation dynamics in strong fields, manipulation of molecules using intense, ultrashort laser pulses and attosecond physics.

Nora G. Kling was born in Dell Rapids, SD, USA. She received the B.A. degree in chemistry and math from Augustana College, Sioux Falls, SD, USA. She received the Master's degree in experimental physics from Kansas State University,Manhattan, KS, USA, in 2009. In 2013, she received the Ph.D. degree with Dr. I. Ben-Itzhak from Kansas State University. In 2009–2010, she worked at the Max Planck Institute for Quantum Optics on a Fulbright stipend. Since 2014, she has been working at the Ludwig Maximilian University of Munich, where she carries out experiments to study ultrafast strong-field processes in atoms and molecules.

Christian Burger was born in Berlin, Germany. He received the Master of Science degree from the Ludwig-Maximilians University of Munich, Germany, in 2013, where since 2013, he has been working toward the Ph.D. degree.

His research interest includes the ionization and dissociation of polyatomic molecules in strong ultrashort laser fields.

Matthias F. Kling received the Ph.D. degree from the University of Göttingen, Göttingen, Germany, in 2002. Afterward, he worked as a postdoctoral researcher at the University of California in Berkeley and at AMOLF in Amsterdam and became a Research Group Leader at the Max Planck Institute of Quantum Optics in 2007. In 2009, he assumed an Assistant Professor at the Kansas-State University. Since 2013, he has been an Associate Professor at the Ludwig-Maximilians University of Munich and heads the "Ultrafast Nanophotonics" group. He is an author and coauthor of more than 110 research papers, a few book chapters, and Co-editor of the book *Attosecond Nanophysics: From Basic Science to Applications* (Wiley, 2015). His research interests include correlated and collective electron dynamics in atoms, molecules and nanostructures in strong and ultrashort laser fields.